Journal of Colloid and Interface Science 510 (2018) 86–94

Contents lists available at ScienceDirect

Journal of Colloid and Interface Science

journal homepage: www.elsevier.com/locate/jcis

Regular Article

In situ crosslinking of surface-initiated ring opening metathesis polymerization of polynorbornene for improved stability

Ishan A. Fursule [a], Ashkan Abtahi [b,c], Charles B. Watkins Jr. [a], Kenneth R. Graham [b], Brad J. Berron [a,*]

[a] Department of Chemical and Materials Engineering, 177 F Paul Anderson Tower, University of Kentucky, Lexington, KY 40506, USA
[b] Department of Chemistry, 161 Jacobs Science Building, University of Kentucky, Lexington, KY 40506, USA
[c] Department of Physics & Astronomy, 177 Chemistry-Physics Building, University of Kentucky, Lexington, KY 40506, USA

GRAPHICAL ABSTRACT

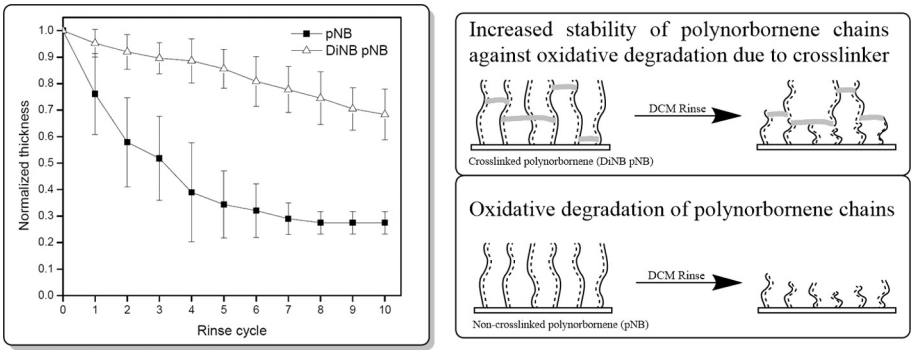

ARTICLE INFO

Article history:
Received 29 June 2017
Revised 12 September 2017
Accepted 13 September 2017
Available online 14 September 2017

Keywords:
Surface-initiated ring opening metathesis polymerization
ROMP
Norbornene
Crosslinker
Oxidative degradation
Film stability
Polynorbornene

ABSTRACT

Hypothesis: In situ crosslinking is expected to increase the solvent stability of coatings formed by surface-initiated ring opening metathesis polymerization (SI ROMP). Solvent-associated degradation limits the utility of SI ROMP coatings. SI ROMP coatings have a unique capacity for post-functionalization through reaction of the unsaturated site on the polymer backbone. Any post-reaction scheme which requires a liquid solvent has the potential to degrade the coating and lower the thickness of the resulting film.
Experiments: We designed a macromolecular crosslinking group based on PEG dinorbornene. The PEG length is tailored to the expected mean chain to chain distance during surface-initiated polymerization. This crosslinking macromer is randomly copolymerized with norbornene through SI ROMP on a gold coated substrate. The solvent stability of polynorbornene coatings with and without PEG dinorbornene is quantitatively determined, and the mechanism of degradation is further supported through XPS and AFM analyses.
Findings: The addition of the 0.25 mol% PEG dinorbornene significantly increases the solvent stability of the SI ROMP coatings. The crosslinker presence in the more stable films is supported with observable PEG absorbances by FTIR and an increase in contact angle hysteresis when compared to non-crosslinked coatings. The oxidation of the SI ROMP coatings is supported by the observation of carbonyl oxygen in the polynorbornene coatings. The rapid loss of the non-crosslinked SI ROMP coating corresponds to nanoscale pitting across the surface and micron-scale regions of widespread film loss. The crosslinked coatings have uniform nanoscale pitting, but the crosslinked films show no evidence of micron-scale film damage. In all, the incorporation of minimal crosslinking content is a simple strategy for improving the solvent stability of SI ROMP coatings.

* Corresponding author.
E-mail addresses: iafu222@g.uky.edu (I.A. Fursule), a.abtahi@uky.edu (A. Abtahi), charles.watkinsuky@gmail.com (C.B. Watkins Jr.), kenneth.graham@uky.edu (K.R. Graham), brad.berron@uky.edu (B.J. Berron).

http://dx.doi.org/10.1016/j.jcis.2017.09.050
0021-9797/

1. Introduction

Functionalized polymer coatings are pervasive throughout the scientific literature, including applications as self-healing materials [1,2], dielectric layers [3–5], responsive materials [6,7], membrane modifiers [8], insulating barriers [9] and conductive surfaces [10]. In particular, surface-initiated polymerization (SIP) techniques [3,11–13] are attractive owing to fine control over growth rate [3,14] and a capacity to create a conformal coating over complex morphologies [12,15,16]. While many surface properties are accessible through SIP of appropriate monomers, the post-polymerization functionalization of a coating provides an opportunity for more diverse surface chemistries than are presently attainable. For example, many ionomer systems are based on polymers which are both fluorinated and sulfonated [17]. A surface-initiated strategy to combine these functional groups requires polymerization followed by sulfonation to avoid the low polymerization rates of sulfonated monomers [18–20].

Of the SIP approaches, surface-initiated ring opening metathesis polymerization (SI ROMP) offers the simplest approach for post-polymerization modification through the unsaturated bonds in polymer backbone [14,21,22]. While most polymerization routes consume the alkene group, SI ROMP opens strained ring monomers by a metathesis catalyst which rearranges and preserves the alkene [14,21,23]. When using ruthenium based metathesis catalysts, SI ROMP can be performed in ambient environmental conditions with a high rate of polymerization and precise control over surface coating thickness [11,24]. In addition, ROMP is faster than other SIP methods like surface initiated atom transfer radical polymerization or surface initiated reversible addition-fragmentation chain transfer polymerization [25–28]. ROMP can produce micron thick coatings in minutes where as other SIP methods typically require hours.

The instability of the SI ROMP coatings represents a critical obstacle in post-modification reactions. Lerum and Chen first observed the decrease in the thickness of these SI ROMP coatings during exposure to the organic solvents (Fig. 1A, B) [29]. They observed a 93% loss in film thickness following exposure of polybutadiene (PBd) to dichloromethane in an ambient atmosphere [29]. The stability of the silane linkage to the SiO_2 substrates indicated damage to the polymer coating layer. By contrasting the film loss upon solvent rinsing in ambient conditions to loss in a nitrogen environment, they proposed that the damage is the result of oxidative cleavage of the internal alkene in the ROMP backbone. As this oxidation is not commonly observed in solution phase ROMP chains, they proposed an entropic driving force to promote the cleavage of a surface-tethered chain. Other groups have also observed a decrease in SI ROMP coating thickness following exposure to organic solvents [19,30–32]. For any solution phase processing of these coatings, film loss during solvation is a critical concern. This challenge is highlighted in a previous study of the sulfonation of SI ROMP coatings. The instability of the coating resulted significant film loss during the solution phase reaction, ultimately requiring thicker initial films to achieve target thickness of the sulfonated film [19].

In the present study, we hypothesize that a crosslinking additive will improve the stability of SI ROMP coatings during solvent exposure and chemical functionalization of the deposited grown coatings. We designed a simple crosslinking molecule for ROMP polymerization consisting of a dinorbornene polyethylene glycol (PEG), and we studied changes to an SI ROMP polynorbornene (pNB) coating with and without incorporation of this crosslinker (Fig. 2). The solvent stabilities of pNB and crosslinked polynorbornene (DiNB-pNB) coatings were contrasted via repetitive exposure to dichloromethane, where minimal film loss was observed for crosslinked coating as compared to the non-crosslinked coating.

Our general approach illustrates a straightforward strategy for stabilizing SI ROMP coatings against solvation-induced degradation to facilitate complex coating chemistries. SI ROMP is a highly utilized coating technique for rapid, conformal coatings on complex surfaces. To date, nitrogen purging has been the only published approach to stabilize SI ROMP coatings to solvent accelerated degradation [29]. We anticipate these crosslinked, solvent stable SI ROMP coatings to be ideal for modification of the olefin backbone in thiol-ene click reactions [33–35]. This pairing of a highly specific, orthogonal click-type reaction and rapid growth of a stable film is expected to enable a diverse class of thick, conformal coatings containing with difficult to polymerize functional groups.

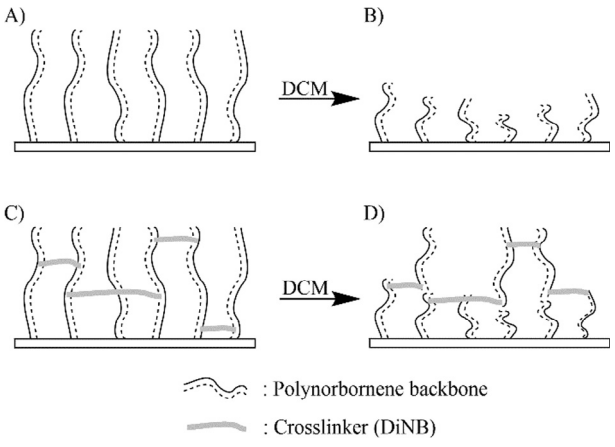

Fig. 1. The role of crosslinking in stabilizing an SI ROMP coating. (A) Non-crosslinked polynorbornene film structure. (B) Non-crosslinked polynorbornene backbone after washing with dichloromethane (DCM). (C) Crosslinked polynorbornene film structure. (D) Crosslinked polynorbornene backbone after washing with dichloromethane.

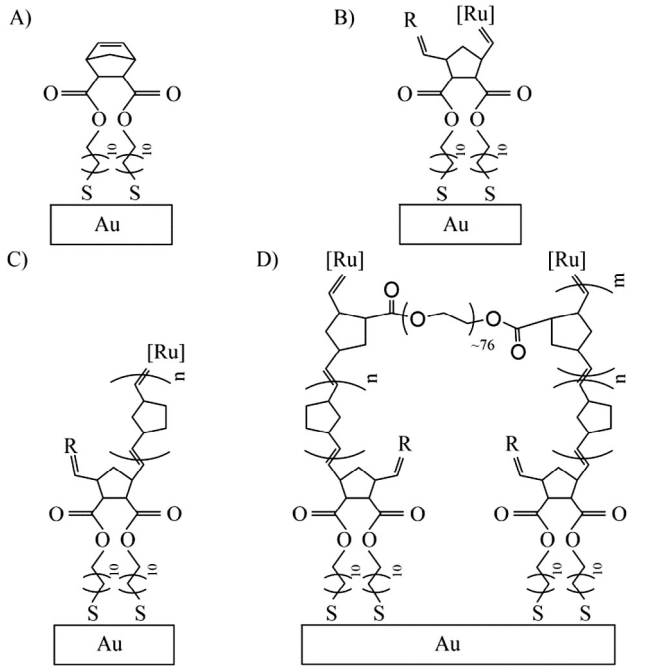

Fig. 2. Schematic representation of crosslinked SI ROMP coating preparation. (A) Norbornenyl ($NBCl_2$) decorated SAM, (B) Grubbs catalyst attached to norbornenyl surface, (C) SI ROMP of polynorbornene, (D) SI ROMP of crosslinked polynorbornene through random co-polymerization.

2. Experimental section

2.1. Materials

Polyethylene glycol 3350 (PEG 3350), 5-norbornene-2-carboxylic acid (NBAC), N,N'-dicyclohexylcarbodiimide (DCC), 4-(dimethylamino) pyridine (DMAP), pyridine, sodium chloride, sodium hydroxide, glycine, 11-mercapto-1-undecanol, trans-3,6-endomethylene-1,2,3,6-tetrahydropthaloyl chloride 97% ($NBCl_2$), Grubbs 1st generation catalyst and bicyclo[2.2.1]hept-2ene (norbornene) were ordered from Sigma Aldrich. All solvents were order from Acros (Fisher) and were used as received.

2.2. Gold coated substrate preparation

Hummer 8.1 DC sputter system was used to sequentially sputter a 200 Å thick adhesion layer of chromium and an 800 Å thick layer of gold on plasma cleaned silicon wafers. The coated wafers were then annealed at 220 °C for at least 1 h to obtain uniform gold surface. The gold substrates were typically cut to 1 cm × 3 cm, rinsed with 200 proof ethanol, and dried under a stream of nitrogen.

2.3. Synthesis of dinorbornene-crosslinker (DiNB)

Dinorbornene-crosslinker was synthesized by referring the protocol by Rehmann et al. [36] (Fig. 3B). Two different solutions were made using degassed dichloromethane (DCM). First, 0.574 mg of DCC and 0.681 mL of NBAC was mixed in 50 mL of DCM under nitrogen environment. Second, a solution consisting of 0.017 g PEG3350 and 0.933 g DMAP was mixed in 50 mL of DCM in a nitrogen environment. After 20 min, 0.225 mL pyridine was added to the PEG solution, and then the PEG solution was added to the NBAC solution in a nitrogen environment and stirred overnight. The product solution was then filtered under vacuum to separate insoluble dicyclohexylurea from soluble dinorbornene-crosslinker product. The soluble product was recrystallized by concentrating the solution under vacuum, and then adding 10 times volume excess of cold diethyl ether. The supernatant ether was discarded and the precipitate was dissolved in chloroform. This solution was then washed twice with aqueous solutions of 0.05 M glycine, 0.05 M sodium hydroxide, and 0.05 M sodium chloride. Finally, the organic solution was washed with 5.1 M solution of sodium chloride. The product was recrystallized again and washed with 10 times volume excess of cold ether and centrifuged to separate the final product. A 400 MHz Varian Nuclear magnetic resonance (NMR) spectroscope was used confirm the composition of the PEG dinorbornene crosslinker. A minimum of 32 scans were used for quantitative determination of peak position and integration. H NMR ($CDCl_3$): δ = 2.9, 3.04, 3.22 (4H, m, >C*H*—CH=), δ = 1.3–1.47(4H, m, >CH—CH_2—CH<), δ = 5.94, 6.1, 6.14, 6.19(4H, m, —C*H*=), δ = 2.26, 2.97(2H, m, >C*H*—CO—), δ = 1.27, 1.53, 1.85–1.97(4H, m, —CH_2—CH—CO), δ = 3.46, 3.63, 3.81, 4.17, 4.25(4H, m, O—CH_2—CH_2—).

2.4. Surface-initiated ring opening metathesis polymerization

Gold coated substrates were placed in 1 mM solution of 11-mercapto-1-undecanol in ethanol for at least 60 min to form a crude, hydroxyl-terminated, self-assembled monolayer. Samples were rinsed with ethanol and dried under a stream of ultra-high purity (UHP) nitrogen. Monolayer coated substrates were exposed to a 5 mM solution of trans-3,6-endomethylene-1,2,3,6-tetrahydropthaloyl chloride ($NBCl_2$) in DCM for 30 min, yielding a norbornene functionalized surface [19]. Samples were rinsed with ethanol and dried under a stream of nitrogen. Grubbs catalyst was immobilized on these substrates by immersing them in 5 mM solution of Grubbs 1st generation catalyst in DCM for 15 min. After 15 min, they were washed with DCM to remove unbound catalyst from the surface. Catalyst coated substrates were immediately put in a norbornene-based monomer solution for SI ROMP. Control surfaces of SI ROMP pNB were prepared with a 0.5 M solution of norbornene (NB) in DCM. Crosslinked SI ROMP surfaces were prepared through incorporation of up to 1 mol% of the DiNB crosslinker. Reaction time was adjusted to control coating thickness. Reaction times ranged from a few seconds to 2 h.

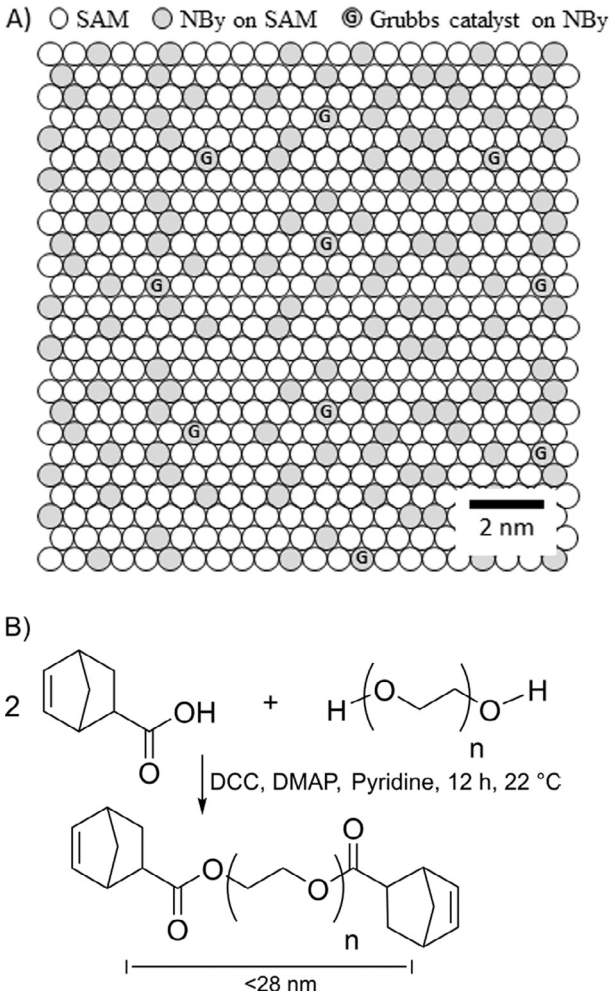

Fig. 3. Relationship between polymer backbone density and dinorbornene linker length. (A) Schematic representing the density of catalyst-related molecules in SI ROMP from a hydroxyl terminated SAM. (B) Synthesis and all-trans length scale for the dinorbornene crosslinker.

2.5. Characterization techniques

A Rame-Hart contact angle goniometer (Model 100) was used to measure the advancing and receding contact angle between on polymer coated surfaces at room temperature. A drop of about 5 μL was placed on the surface and measurements were performed by increasing or decreasing drop volume to advance or recede the air-water-solid interface across the surface. The data is reported as mean ± standard deviation of at least 8 samples.

An Agilent 680 Fourier transform infrared spectrometer with an MCT external detector was used for compositional analysis of polymer surface coatings. The instrument was equipped with a

Universal Sampling Accessory for grazing angle analysis of thin polymer coatings on metal surfaces. The p-polarized IR beam was reflected off the surface at an 80° angle from the surface normal. 100 scans of background and each sample were performed at resolution of 4 cm^{-1}.

A profilometer was used to determine film thickness. The polymer coating was scratched with a wooden pick while the underlying gold coated silicon substrate was unaffected. A Dektak6m programmable surface profiler measuring system was used to measure the scratch depth at an applied force of 3 mg and a 1.000 mm scan length.

Electrochemical impedance spectroscopy was performed using a standard three-electrode flat cell (Princeton Applied Research, model K0235) and a Gamry Reference 600 potentiostat. The substrates were mounted on the flat cell with a fixed working electrode area of 1 cm^2. The polymer coated sample was used as a working electrode in combination with a Ag/AgCl/saturated KCl (aq.) reference electrode and a bare gold coated silicon substrate counter electrode in an electrolyte solution of 1 mM $K_3[Fe(CN)_6]$, 1 mM $K_4[Fe(CN)_6]$ and 0.1 M Na_2SO_4. Spectra were collected between 10^{-1} and 10^4 Hz. A Randles equivalent circuit modified with Warburg Impedance was fit to the collected data to determine the film resistance and capacitance [37]. All experiments were performed at room temperature. All reported data are the mean ± standard deviation of the measurement from at least 8 samples.

Film coverage and surface morphology were investigated with Agilent Technologies 5500 scanning probe molecular imaging AFM instrument. Images of 10 μm × 10 μm are collected in tapping mode with silicon tip.

XPS spectra were collected using X-rays generated by a Mg-K-α source (1253.6 eV, PHI 04-548 Dual Anode X-ray source). Emitted photoelectrons were analyzed with an 11″ diameter hemispherical electron energy analyzer with multichannel detector, with pass energies of 23.5 eV and 0.025 eV step size (Phi 5600). Samples were measured with a 45° take off angle.

3. Results and discussion

The crosslinking monomer design is based on the expected distance between polymer chains in an actively polymerizing SI ROMP surface. In SI ROMP, neighboring chains are anchored to the substrate at locations which are primed by catalyst attachment. The catalyst surface density is dictated by grafting density of $NBCl_2$ and the subsequent grafting of the Grubbs catalyst. Based on estimates of ~10^{12} molecules per cm^2 of Grubbs catalyst in a prior study using a similar catalyst attachment scheme [38], the expected distance between pNB backbone chains to be approximately 4 nm (Fig. 3A). The crosslinker is designed to be of comparable length (or distance between 2 ends of crosslinker) as the distance between chains to encourage intermolecular crosslinking. PEG 3350 is used as a linker for two 5-norbornene-2-carboxylic acid molecules to yield a molecule with an all *trans* end to end distance of ~28 nm. While 28 nm is excessive for crosslinking across chains separated by 4 nm, the solvated structure of the crosslinking chain is significantly smaller than the all *trans* length of molecule. The radius of gyration of PEG in dichloromethane is not readily available. We approximate the radius of gyration of PEG 3350 in dichloromethane to be similar to the radius of gyration of PEG 3350 in water (~2.3 nm) [39]. This estimate of solvated chain length is comparable to that of the distance between initiation sites and is expected to be appropriate for crosslinking this surface-initiated system. Longer crosslinking chains are also expected to crosslink a surface initiated system, but these longer chains are expected to decrease the film growth rate through dilution of the norbornene reactive groups.

3.1. Influence of dinorbornene-crosslinker on SI ROMP coating composition and structure

The incorporation of the crosslinking molecule was confirmed via FTIR. In the spectra for the pNB coatings, distinct methylene peaks were observed for symmetric stretching, asymmetric stretching, and scissoring modes. The C—H stretching region for pNB coating IR spectra has strong cyclic methylene peaks at 2945 cm^{-1} (asymmetric) and at 2862 cm^{-1} (symmetric) with an additional stretching peak at 2907 cm^{-1} [40]. A cyclic methylene scissoring peak is seen at 1455 cm^{-1} with signature Davydov splitting into 1465 cm^{-1} and 1448 cm^{-1} indicating a relatively homogenous and well-ordered chain structure [41]. The out of plane bending peaks for C=CH olefin functionality [40,42] are seen at 968 cm^{-1} and a shoulder-like C=CH stretching peak at 3030 cm^{-1} [40,42].

For pNB coatings grown with the addition of 0.25, 0.5, or 1 mol% DiNB crosslinker, all characteristic peaks for pNB are conserved, and additional peaks consistent with the IR absorbance of PEG are introduced (Fig. 4 and SI – Fig. 3). The finger print region for PEG C—O—C absorption by PEG around 1029 cm^{-1} [43–45] was observed at cross linker concentrations as low as 0.25 mol %. At this minimum concentration, the C=CH out of plane bending peak is in the same position as in non-crosslinked pNB coating suggesting no major changes in the environment of the olefin functionality after crosslinking. The position of the methylene scissoring peaks is similarly conserved at 1465 cm^{-1} and 1446 cm^{-1}. The asymmetric and symmetric methylene C—H stretching peaks (2950 cm^{-1} and 2865 cm^{-1}) are typically sensitive to alterations in polymer crystallinity [46], where these peaks shift by over 10 cm^{-1} with a change in chain-chain interactions [47,48]. The crosslinked pNB is red shifted by 3–5 cm^{-1} when compared to these absorbances in the pure pNB coating. This red shift is supportive of a change in the chain packing with the addition of the DiNB crosslinking monomer. Since our goal is to stabilize SI ROMP films while leaving their functionality intact, we focused the remaining studies on 0.25 mol% DiNB.

The incorporation of the DiNB crosslinker in the pNB coatings is further supported by analysis of the XPS spectra of the films (Fig. 5). When compared to the spectra of the pNB coatings, the spectra of the DiNB-pNB coatings include a shoulder centered at 534.5 eV, consistent with the ethereal oxygen in the PEG functionality of the DiNB crosslinker [49,50]. The XPS spectra for both films include peaks at ~533 eV consistent with carbonyl oxygen. Critically, the DiNB-pNB coatings are expected to include <0.1 atom%

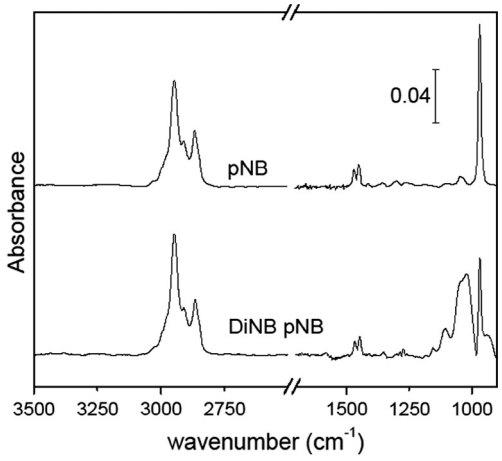

Fig. 4. Reflection absorption infrared spectroscopy of SI ROMP of polynorbornene (pNB) and crosslinked polynorbornene with 0.25 mol % crosslinker (DiNB-pNB).

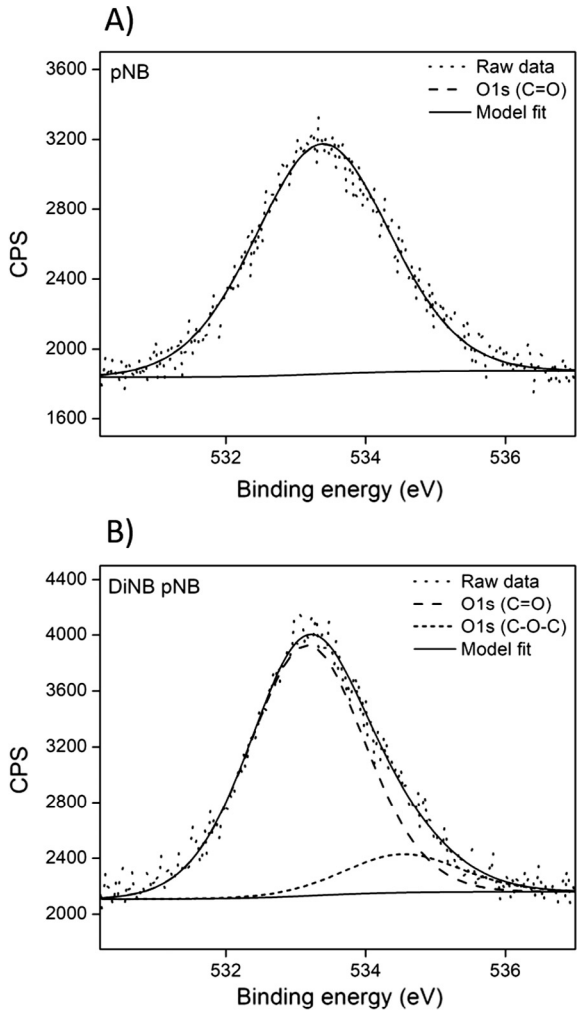

Fig. 5. O1 s region of XPS spectra of (A) non-crosslinked pNB coatings and (B) DiNB-pNB coatings.

carbonyl oxygen from the ester bound norbornene, and the pNB coatings are not expected to contain any oxygen in the bulk polymer layer. The high carbonyl oxygen content of the coatings is consistent with previously observed degradation products of polymers [51]. While Lerum and Chen postulated the entropy accelerated oxidation of SI ROMP pNB coatings, the spectral observation of these degradation products has not been reported to date [29]. The presence of carbonyl oxygen peaks in the XPS spectra strongly supports the oxidative degradation of these coatings in ambient environments.

The rate of film growth is dramatically decreased by the addition of the DiNB crosslinking monomer (Table 1). While a 0.5 M solution of NB in dichloromethane yields a coating of ~1 μm in 15 min, the addition of 0.25 mol% DiNB to the same solution of NB only yields a 30 nm coating. To determine if the decrease in film growth rate is related to chemical attributes of the crosslinker or steric hindrance from the presence of solvated polymer chains, 0.25 mol% methylene terminated PEG (Mn 2000) or 0.25 mol% polystyrene (Mn 2000) was added to the 0.5 M NB solution during

Table 1
Coating thickness following immersion of a Grubbs catalyst coated substrate in the indicated solution for 15 min.

Solution	Thickness (nm)
0.5 M NB in dichoromethane	1046 ± 506
0.5 M NB and 0.25 mol% DiNB in dichoromethane	33 ± 12
0.5 M NB and 0.25 mol% methylene terminated PEG 2000 in dichoromethane	16 ± 7
0.5 M NB and 0.25 mol% polystyrene (Mn 2200)	534 ± 93

Table 2
Advancing and receding contact angle for water on SI ROMP coating. Data represent mean ± standard deviation.

Coating	Thickness (nm)	Θ_A (°)	Θ_R (°)
pNB	46 ± 6	98 ± 2	77 ± 3
DiNB-pNB	40 ± 5	95 ± 3	65 ± 6

Table 3
Film resistance and interfacial capacitance for SI ROMP coating.

Film	Thickness (nm)	Log (R_f) Ω cm^2	C_f nF/cm^2
pNB	38.5 ± 12.4	4.66 ± 0.44	623 ± 514
DiNB-pNB	36 ± 10.5	5.93 ± 0.39	210 ± 108

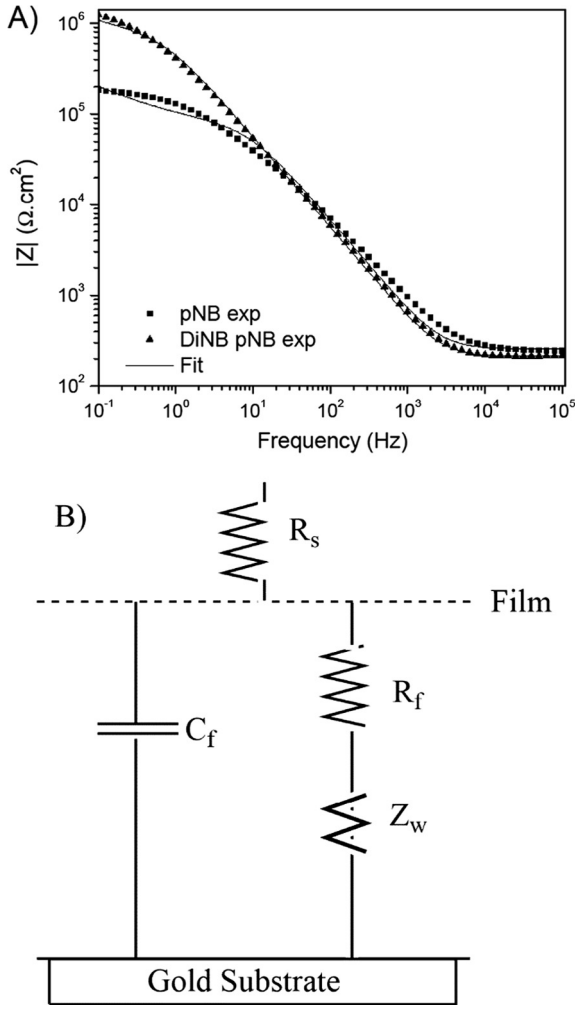

Fig. 6. Electrochemical impedance spectroscopy of SI ROMP polynorbornene coatings. (A) Bode plot of representative experimental data from SI ROMP polynorbornene (■) and SI ROMP crosslinked polynorbornene (▲) coatings. Lines represent fitting of an equivalent circuit to the experimental data. (B) Modified Randle's model circuit with Warburg impedance (Z_w) used to fit experimental data. (R_s: Solution resistance, R_f: Film resistance, C_f: Film capacitance).

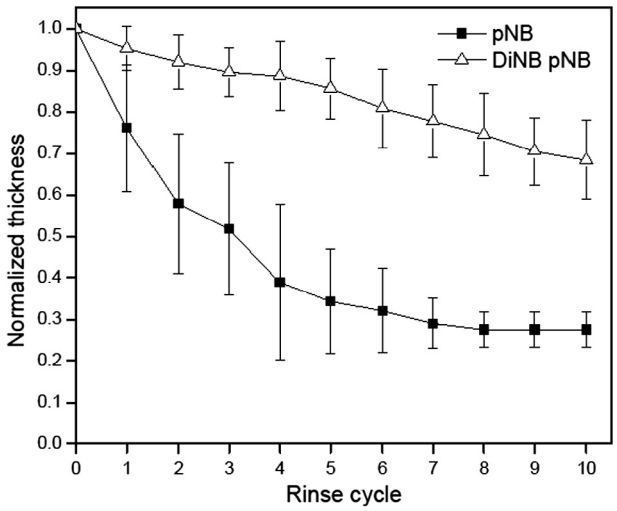

Fig. 7. SI ROMP coating stability data. The profilometric thickness of a polynorbornene or crosslinked polynorbornene coating is measured following the indicated number of rinse cycles. Each rinse cycle is the sequential exposure to DCM, ethanol, and water.

polymerization. While the addition of the PEG limited the film growth to 16 nm, the polystyrene and NB solution still supported film growth >500 nm. These polymer additives both decrease the rate of pNB film growth, but the PEG chain has a stronger negative effect on the film growth rate than the polystyrene. In all, the PEG backbone for the crosslinker is not ideal for supporting the rapid growth of thicker films using Grubbs first generation catalyst. Critically, the polystyrene and other commonly available polymer backbones are more challenging to end functionalize. As a result, we use the PEG backbone here to demonstrate the proof of concept for coating stabilization. For applications requiring thicker films, alternative catalysts or crosslinker chemistries may be warranted.

Advancing and receding water contact angles for pNB coating are ~98° and ~77°, and these values are consistent with prior studies (Table 2) [19,20]. For DiNB-pNB films, the advancing water contact angle is similar (95°) to that of the pNB film. There is a significant decrease in the receding water contact angle (~65°) with the incorporation of the DiNB crosslinker when compared to the pNB film. The decrease in the contact angles are attributed to the introduction of hydrophilic PEG chains in the DiNB crosslinker [47]. Additionally, the larger change in the receding contact angle than for the advancing contact angle is expected, owing to the receding contact angle's greater dependency on the hydrophilic content of the surface [52,53].

Electrochemical impedance spectroscopy was used to evaluate changes in coating structuring upon the addition of the DiNB crosslinker (Table 3). Fig. 6A displays representative Bode plots for ~37 nm pNB coatings and DiNB-pNB coatings. A modified Randle's equivalent circuit with Warburg's impedance term for mass transport resistance was fit to the experimental data. Based on these fits,

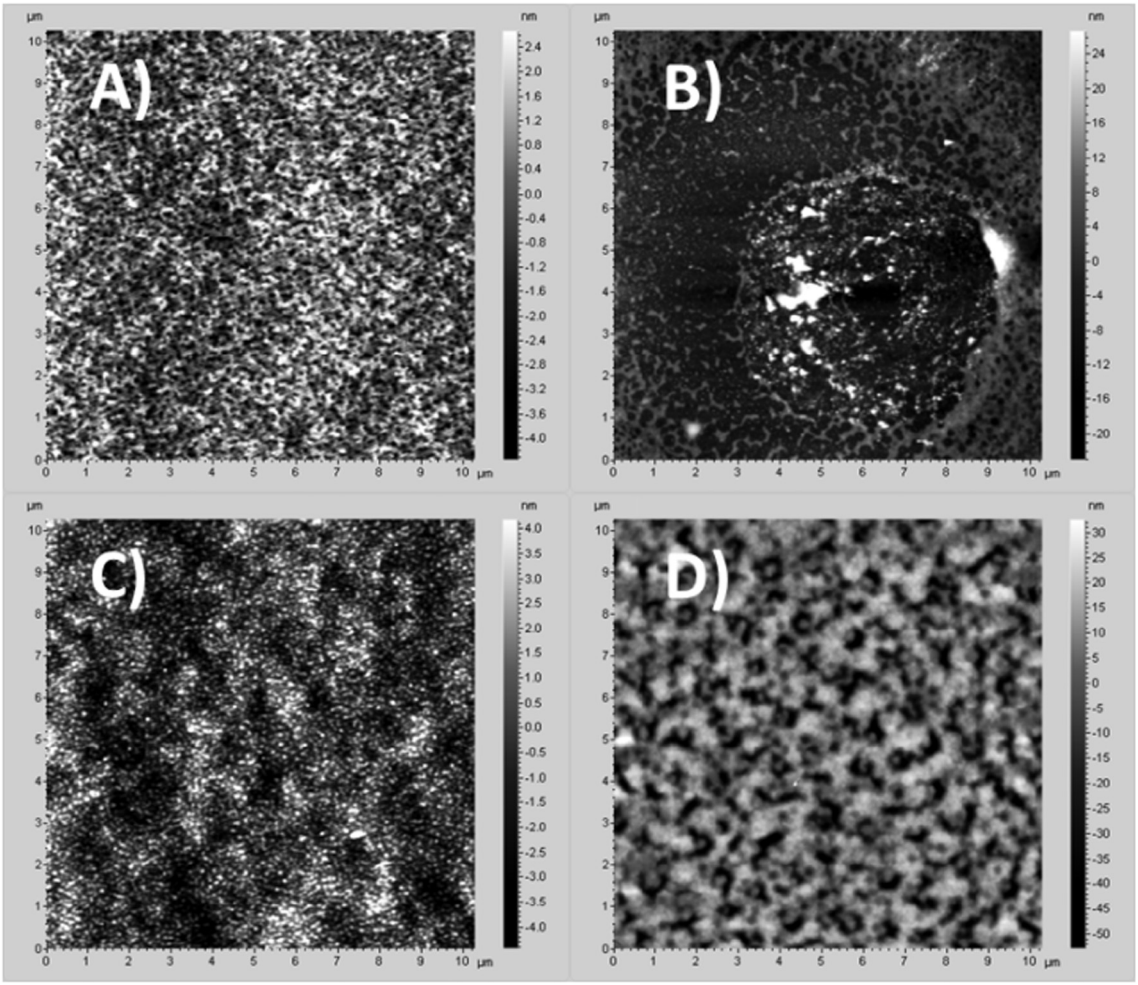

Fig. 8. AFM image of SI ROMP coatings; (A) Non-crosslinked i.e. pNB and unrinsed, (B) Non-crosslinked i.e. pNB and rinsed, (C) Crosslinked i.e. DiNB-pNB and unrinsed, (D) Crosslinked i.e. DiNB-pNB and rinsed.

the film capacitance of the pNB coating (623 ± 514 nF/cm^2) was similar to that of the crosslinked film (210 ± 108 nF/cm^2). This supports a similar dielectric and thickness for the two coatings. Interestingly, the crosslinked coating had a slightly higher mean film resistance ($10^{5.9}$ Ω cm^2) than that of the native pNB coating ($10^{4.7}$ Ω cm^2). While this potentially supports greater coating uniformity in the crosslinked film, this minimal difference in mean resistance will not significantly alter the practical application of a functional SI ROMP coating.

3.2. The influence of crosslinking on coating stability in solvent

To determine the effectiveness of a 0.25 mol% crosslinker in stabilizing an SI ROMP coating, we measured the thickness of pNB and DiNB-pNB coatings after rinsing sequentially with dichloromethane, ethanol, and water (Fig. 7). All the samples were rinsed in the same ambient atmospheric conditions to minimize the variation in temperature and oxygen content in the atmosphere. Each sample was immersed in the DCM for 5 s, removed into ambient air, and gently shaken to remove excess solvent. Samples were then immediately rinsed with ethanol and then water in the same fashion. After rinsing with water, the sample was dried under a stream of nitrogen. Thicker coatings were utilized in this study to allow greater resolution in the fractional coating loss, and polymerization times were adjusted to achieve coatings approximately 90 nm in thickness. The stability of SI ROMP coating increased significantly with the addition of the DiNB crosslinker for the first rinse and each subsequent rinse ($p < 0.05$). The film loss after 10 rinses decreased from ~73% to ~28% after introducing crosslinker. The relative film loss for the pNB coating compares favorably with a prior study by Lerum and Chen, where 93% of a polybutadiene film was lost after 10 rinses of dichloromethane in an ambient environment. A small decrease in the coating thickness upon rinsing still occurs in the DiNB sample, and this film loss is expected due to the persistence of olefin functionality in the polymer backbone.

The microstructure of the rinsed and unrinsed coatings further informs the role of coating crosslinking in the solvent stability of SI ROMP films. Fig. 8 shows the topographical images of pNB and DiNB-pNB coatings obtained by atomic force microscopy (AFM). Immediately after film formation, the pNB and DiNB-pNB coatings look similar to other polymer brush coatings found in literature, including examples of other SI ROMP coatings [14,20,54]. For the pNB film, the surface morphology changes dramatically after exposure to 10 cycles of dichloromethane, ethanol and water. The rinsed pNB coatings (Fig. 8B) have nanoscale pits indicative of a uniform loss of material throughout the coating. Additionally, the rinsed pNB coatings have circular, micron-scale defects Fig. 8B and regions where the pits are interconnected. The DiNB-pNB also forms nanoscale pits from the loss of polymer, but the overall coating morphology is still similar to that of an as-grown pNB and the DiNB-pNB coating. The rinsed DiNB-pNB coating does not have large regions of widespread film loss seen in the pNB rinsed coatings. In all, the film loss in the rinsed pNB coatings supports a rapid, uniform loss of coating material, with localized regions of accelerated film loss. The crosslinked DiNB-pNB coatings still exhibit uniform loss of material on the submicron scale, but the macroscale loss of films is not observed.

4. Conclusion

We hypothesized that in situ crosslinking is a straightforward approach to stabilize SI ROMP coatings. We found that the stability of pNB coating against organic solvents in an ambient environment is increased significantly with the addition of a dinorbornene crosslinker at 0.25 mol%. Additionally, we report the first spectral data supporting oxidative degradation of these SI ROMP coatings in ambient environments. To date, processing in a deoxygenated environment is the only published approach to limit solvent-associated degradation [29]. Interestingly, ROMP with Grubbs catalyst is largely tolerant of oxygen [55,56], where many competing grafting-from chemistries have stricter purging requirements [57,58]. A processing requirement of an oxygen-free environment would greatly decrease the attractiveness of ROMP-based surface modification over slower techniques like SI-ATRP and other radical chain growth strategies [59,60].

We envision utility of these solvent-stable films in the fabrication of conformal coatings of difficult-to-polymerize functional groups. The residual alkene functionality of ROMP coatings is compatible with thiol-based click reactions [34,35]. The selectivity of thiol-ene chemistry makes this approach ideal for a diverse set of functional groups [61,62], and the oxygen tolerance of thiol-ene chemistry also is appropriate for ambient processing of a thick, solvent-stable ROMP coatings [63–65]. The great diversity of functional norbornenes [66,67] also creates an opportunity for one functional group to be polymerized on a norbornene side chain with a second functional group to be added via thiol-ene chemistry on the polymer backbone. Our demonstration of an ambient environment, solvent-tolerant SI ROMP strategy enables the development of more complex surface tethered polymer chemistries for functional coatings.

The crosslinker design described here is based on a PEG-dinorbornene molecule of sufficient length to bridge adjacent active sites on the catalyst primed surface. The PEG chemistry was selected primarily for ease of functionalization, but was discovered to strongly decrease the rate of polymerization for the pNB coatings. Additionally, the total amount of crosslinker was limited to 0.25 mol% of the NB in solution due to the lower growth rate in the presence of PEG. In future work, the use of catalysts with greater functional group tolerance is expected to enable the use of this PEG dinorbornene crosslinker with a less detrimental impact on the film growth rate. Alternatively, the crosslinker may be redesigned to utilize a backbone more compatible with Grubbs first generation catalyst. While we expect greater stability with higher crosslinker loadings, we also demonstrated that the crosslinker alters the wettability of the polymer coating. A higher crosslinker loading is expected to have a greater impact on the surface properties of the coating. As a result, future studies in functional SI ROMP coatings should carefully consider the crosslinker's interaction with the catalyst, the crosslinker's impact on the desired surface properties, and the desired solvent stability of the coating.

Acknowledgement

We thank the University of Kentucky, Department Of Chemistry for providing access to the Nuclear Magnetic Resonance facility. We also acknowledge University of Kentucky Center for Nanoscale Science and Engineering for the use of the sputtering machine and profilometer.

Funding

This work was supported by the National Science Foundation [Grant No. CMMI-1334403]. Acknowledgment is made to the Donors of the American Chemical Society Petroleum Research Fund [52743-DNI5 and 57619-DNI10] for partial support of this research.

Appendix A. Supplementary material

Supplementary data associated with this article can be found, in the online version, at http://dx.doi.org/10.1016/j.jcis.2017.09.050.

References

[1] S.R. Sriram, Development of self-healing polymer composites and photoinduced ring-opening metathesis polymerization. (2002).
[2] B. Briscoe, L. Fiori, E. Pelillo, Nano-indentation of polymeric surfaces, J. Phys. D Appl. Phys. 31 (19) (1998) 2395.
[3] I.M. Rutenberg et al., Synthesis of polymer dielectric layers for organic thin film transistors via surface-initiated ring-opening metathesis polymerization, J. Am. Chem. Soc. 126 (13) (2004) 4062–4063.
[4] N.R. Grove et al., Functionalized polynorbornene dielectric polymers: adhesion and mechanical properties, J. Polym. Sci. Part B: Polym. Phys. 37 (21) (1999) 3003–3010.
[5] Y. Bai et al., Photosensitive polynorbornene based dielectric. I. Structure–property relationships, J. Appl. Polym. Sci. 91 (5) (2004) 3023–3030.
[6] D. Bai, B.M. Habersberger, G.K. Jennings, pH-responsive copolymer films by surface-catalyzed growth, J. Am. Chem. Soc. 127 (47) (2005) 16486–16493.
[7] N. Ayres, S.G. Boyes, W.J. Brittain, Stimuli-responsive polyelectrolyte polymer brushes prepared via atom-transfer radical polymerization, Langmuir 23 (1) (2007) 182–189.
[8] A.M. Balachandra, G.L. Baker, M.L. Bruening, Preparation of composite membranes by atom transfer radical polymerization initiated from a porous support, J. Membr. Sci. 227 (1–2) (2003) 1–14.
[9] C.J. Faulkner, P. Andrew Payne, G.K. Jennings, Surface-initiated ring-opening metathesis polymerization of 5-(perfluorohexyl)norbornene on carbon paper electrodes, J. Colloid Interface Sci. 351 (1) (2010) 248–253.
[10] S. Voccia et al., Sequential electrografting and ring-opening metathesis polymerization: a strategy for the tailoring of conductive surfaces, Macromol. Rapid Commun. 26 (10) (2005) 779–783.
[11] S. Edmondson, V.L. Osborne, W.T. Huck, Polymer brushes via surface-initiated polymerizations, Chem. Soc. Rev. 33 (1) (2004) 14–22.
[12] M.R. Buchmeiser, Polymeric monolithic materials: syntheses, properties, functionalization and applications, Polymer 48 (8) (2007) 2187–2198.
[13] M.A. Jordi, T.A. Seery, Quantitative determination of the chemical composition of silica-poly (norbornene) nanocomposites, J. Am. Chem. Soc. 127 (12) (2005) 4416–4422.
[14] N.Y. Kim et al., Surface-initiated ring-opening metathesis polymerization on Si/SiO2, Macromolecules 33 (8) (2000) 2793–2795.
[15] G.K. Jennings, E.L. Brantley, Physicochemical properties of surface-initiated polymer films in the modification and processing of materials, Adv. Mater. 16 (22) (2004) 1983–1994.
[16] S.G. Boyes et al., Synthesis, characterization, and properties of ABA type triblock copolymer brushes of styrene and methyl acrylate prepared by atom transfer radical polymerization, Macromolecules 35 (13) (2002) 4960–4967.
[17] Y.L. Liu et al., Surface-initiated atom transfer radical polymerization from porous poly (tetrafluoroethylene) membranes using the C F groups as initiators, J. Polym. Sci. Part A: Polym. Chem. 48 (10) (2010) 2076–2083.
[18] B.J. Berron et al., Surface-initiated growth of ionomer films from Pt-Modified gold electrodes, Langmuir 25 (21) (2009) 12721–12728.
[19] B.J. Berron, P.A. Payne, G.K. Jennings, Sulfonation of surface-initiated polynorbornene films, Ind. Eng. Chem. Res. 47 (20) (2008) 7707–7714.
[20] B.J. Berron, E.P. Graybill, G.K. Jennings, Growth and structure of surface-initiated poly(n-alkylnorbornene) films, Langmuir 23 (23) (2007) 11651–11655.
[21] M. Weck et al., Ring-opening metathesis polymerization from surfaces, J. Am. Chem. Soc. 121 (16) (1999) 4088–4089.
[22] A. Leitgeb, J. Wappel, C. Slugovc, The ROMP toolbox upgraded, Polymer 51 (14) (2010) 2927–2946.
[23] C.W. Bielawski, R.H. Grubbs, Highly efficient ring-opening metathesis polymerization (ROMP) using new ruthenium catalysts containing N-heterocyclic carbene ligands, Angew. Chem. Int. Ed. 39 (16) (2000) 2903–2906.
[24] C.W. Bielawski, R.H. Grubbs, Increasing the initiation efficiency of ruthenium-based ring-opening metathesis initiators: effect of excess phosphine, Macromolecules 34 (26) (2001) 8838–8840.
[25] L. Zeng et al., A new approach for synthesis of the comb-shaped poly (ε-caprolactone) brushes on the surface of nano-hydroxyapatite by combination of ATRP and ROP, J. Colloid Interface Sci. 352 (1) (2010) 36–42.
[26] D. Xu et al., Functionalization of hydrogen-terminated silicon via surface-initiated atom-transfer radical polymerization and derivatization of the polymer brushes, J. Colloid Interface Sci. 279 (1) (2004) 78–87.
[27] X. Chen et al., Synthesis and aqueous solution properties of polyelectrolyte-grafted silica particles prepared by surface-initiated atom transfer radical polymerization, J. Colloid Interface Sci. 257 (1) (2003) 56–64.
[28] M. Zhang et al., Double-responsive polymer brushes on the surface of colloid particles, J. Colloid Interface Sci. 301 (1) (2006) 85–91.
[29] M.F.Z. Lerum, W. Chen, Acute degradation of surface-bound unsaturated polyolefins in common solvents under ambient conditions, Langmuir 25 (19) (2009) 11250–11254.
[30] A.J. Sipinen, D.R. Rutherford, A study of the oxidative degradation of polyolefins, J. Environ. Polym. Degrad. 1 (3) (1993) 193–202.
[31] C.J. Faulkner, R.E. Fischer, G.K. Jennings, Surface-initiated polymerization of 5-(Perfluoro-n-alkyl)norbornenes from gold substrates, Macromolecules 43 (3) (2010) 1203–1209.
[32] M.F.Z. Lerum, W. Chen, Surface-initiated ring-opening metathesis polymerization in the vapor phase: an efficient method for grafting cyclic olefins with low strain energies, Langmuir 27 (9) (2011) 5403–5409.
[33] C.E. Hoyle, T.Y. Lee, T. Roper, Thiol-enes: chemistry of the past with promise for the future, J. Polym. Sci. Part a – Polym. Chem. 42 (21) (2004) 5301–5338.
[34] C.E. Hoyle, C.N. Bowman, Thiol-Ene Click Chemistry, Angew. Chem. - Int. Ed. 49 (9) (2010) 1540–1573.
[35] C.E. Hoyle, A.B. Lowe, C.N. Bowman, Thiol-click chemistry: a multifaceted toolbox for small molecule and polymer synthesis, Chem. Soc. Rev. 39 (4) (2010) 1355–1387.
[36] M.S. Rehmann, A.C. Garibian, A.M. Kloxin, Hydrolytically degradable thiol–ene hydrogels for protein release, in: Macromolecular Symposia, Wiley Online Library. 2013.
[37] T.M. Nahir, E.F. Bowden, Impedance spectroscopy of electroinactive thiolate films adsorbed on gold, Electrochim. Acta 39 (16) (1994) 2347–2352.
[38] C.A. Escobar et al., Amplification of surface-initiated ring-opening metathesis polymerization of 5-(Perfluoro-n-alkyl)norbornenes by macroinitiation, Langmuir 29 (40) (2013) 12560–12571.
[39] N. Ziebacz et al., Crossover regime for the diffusion of nanoparticles in polyethylene glycol solutions: influence of the depletion layer, Soft Matter 7 (16) (2011) 7181–7186.
[40] J. Planche, A. Revillon, A. Guyot, Chemical modification of polynorbornene. I. sulfonation in dilute solution, J. Polym. Sci., Part A: Polym. Chem. 26 (2) (1988) 429–444.
[41] D.S.M. de Silva et al., Chain tilt and surface disorder in lamellar crystals. A FTIR and SAXS study of labeled long alkanes, Macromolecules 35 (20) (2002) 7730–7741.
[42] R.M. Silverstein et al., Spectrometric Identification of Organic Compounds, John Wiley & Sons. 2014.
[43] J.J. Sahlin, N.A. Peppas, Near-field FTIR imaging: a technique for enhancing spatial resolution in FTIR microscopy, J. Appl. Polym. Sci. 63 (1) (1997) 103–110.
[44] M. Roberts, M. Bentley, J. Harris, Chemistry for peptide and protein PEGylation, Adv. Drug Deliv. Rev. 64 (2012) 116–127.
[45] T.J. Singh, S. Bhat, Morphology and conductivity studies of a new solid polymer electrolyte:$(PEG)_xLiClO_4$, Bull. Mater. Sci. 26 (7) (2003) 707–714.
[46] J. Weber, P.C. Beard, S.E. Bohndiek, Contrast agents for molecular photoacoustic imaging, Nat. Meth. 13 (8) (2016) 639–650.
[47] C.A. Stevens, L. Safazadeh, B.J. Berron, Thiol-yne adsorbates for stable, low-density, self-assembled monolayers on gold, Langmuir 30 (8) (2014) 1949–1956.
[48] L. Safazadeh, B.J. Berron, Photopatterning of stable, low-density self-assembled monolayers on gold, Langmuir 31 (9) (2015) 2689–2696.
[49] P. Dietrich et al., An anchoring strategy for photoswitchable biosensor technology: azobenzene-modified SAMs on Si (111), Appl. Phys. A Mater. Sci. Process. 93 (2) (2008) 285–292.
[50] A. Papra, N. Gadegaard, N.B. Larsen, Characterization of ultrathin poly (ethylene glycol) monolayers on silicon substrates, Langmuir 17 (5) (2001) 1457–1460.
[51] J. White, A. Turnbull, Weathering of polymers: mechanisms of degradation and stabilization, testing strategies and modelling, J. Mater. Sci. 29 (3) (1994) 584–613.
[52] J. Drelich et al., Contact angles for liquid drops at a model heterogeneous surface consisting of alternating and parallel hydrophobic/hydrophilic strips, Langmuir 12 (7) (1996) 1913–1922.
[53] J. Drelich, J.D. Miller, R.J. Good, The effect of drop (bubble) size on advancing and receding contact angles for heterogeneous and rough solid surfaces as observed with sessile-drop and captive-bubble techniques, J. Colloid Interface Sci. 179 (1) (1996) 37–50.
[54] Q. Ye et al., Surface-initiated ring-opening metathesis polymerization of pentadecafluorooctyl-5-norbornene-2-carboxylate from variable substrates modified with sticky biomimic initiator, Macromolecules 43 (13) (2010) 5554–5560.
[55] S.T. Nguyen et al., Ring-opening metathesis polymerization (Romp) of norbornene by a group-Viii carbene complex in protic media, J. Am. Chem. Soc. 114 (10) (1992) 3974–3975.
[56] S.T. Nguyen, R.H. Grubbs, J.W. Ziller, Syntheses and activities of new single-component, ruthenium-based olefin metathesis catalysts, J. Am. Chem. Soc. 115 (21) (1993) 9858–9859.
[57] K. Matyjaszewski et al., Polymers at interfaces: using atom transfer radical polymerization in the controlled growth of homopolymers and block copolymers from silicon surfaces in the absence of untethered sacrificial initiator, Macromolecules 32 (26) (1999) 8716–8724.
[58] E.L. Brantley, T.C. Holmes, G.K. Jennings, Modification of ATRP surface-initiated poly(hydroxyethyl methacrylate) films with hydrocarbon side chains, J. Phys. Chem. B 108 (41) (2004) 16077–16084.
[59] Q. Huang et al., Surface functionalized SiO_2 nanoparticles with cationic polymers via the combination of mussel inspired chemistry and surface initiated atom transfer radical polymerization: characterization and enhanced removal of organic dye, J. Colloid Interface Sci. 499 (2017) 170–179.
[60] T.V. Charpentier et al., Development of anti-icing materials by chemical tailoring of hydrophobic textured metallic surfaces, J. Colloid Interface Sci. 394 (2013) 539–544.
[61] L.M. Campos et al., Development of thermal and photochemical strategies for thiol-ene click polymer functionalization, Macromolecules 41 (19) (2008) 7063–7070.
[62] K.L. Killops, L.M. Campos, C.J. Hawker, Robust, efficient, and orthogonal synthesis of dendrimers via thiol-ene click chemistry, J. Am. Chem. Soc. 130 (15) 2008 5062–5064.

[63] K.S. Anseth, C.M. Wang, C.N. Bowman, Kinetic evidence of reaction diffusion during the polymerization of multi (meth) acrylate monomers, Macromolecules 27 (3) (1994) 650–655.
[64] N.B. Cramer, C.N. Bowman, Kinetics of thiol–ene and thiol–acrylate photopolymerizations with real-time fourier transform infrared, J. Polym. Sci. Part A: Polym. Chem. 39 (19) (2001) 3311–3319.
[65] M.S. Rehmann, A.C. Garibian, A.M. Kloxin, Hydrolytically degradable thiol–ene hydrogels for protein release, Macromol. Symposia 329 (1) (2013) 58–65.
[66] J. Sauer, R. Sustmann, Mechanistic aspects of Diels-Alder reactions – a critical survey, Angew. Chem. – Int. Ed. Eng. 19 (10) (1980) 779–807.
[67] A.J. Pasquale, A.R. Fornof, T.E. Long, Synthesis of norbornene derivatives by Diels-Alder cycloaddition and subsequent copolymerization with maleic anhydride, Macromol. Chem. Phys. 205 (5) (2004) 621–627.